# Optical Properties of Internally Mixed Aerosol Particles Composed of Dicarboxylic Acids and Ammonium Sulfate

**Miriam A. Freedman,[†] Christa A. Hasenkopf,[†,‡] Melinda R. Beaver,[†,§,#] and Margaret A. Tolbert*[,†,§]**

*Cooperative Institute for Research in Environmental Sciences (CIRES), Department of Atmospheric and Oceanic Sciences, and Department of Chemistry and Biochemistry, University of Colorado Boulder, Colorado 80309*

*Received: July 2, 2009; Revised Manuscript Received: September 5, 2009*

We have investigated the optical properties of internally mixed aerosol particles composed of dicarboxylic acids and ammonium sulfate using cavity ring-down aerosol extinction spectroscopy at a wavelength of 532 nm. The real refractive indices of these nonabsorbing species were retrieved from the extinction and concentration of the particles using Mie scattering theory. We obtain refractive indices for pure ammonium sulfate and pure dicarboxylic acids that are consistent with literature values, where they exist, to within experimental error. For mixed particles, however, our data deviates significantly from a volume-weighted average of the pure components. Surprisingly, the real refractive indices of internal mixtures of succinic acid and ammonium sulfate are higher than either of the pure components at the highest organic weight fractions. For binary internal mixtures of oxalic or adipic acid with ammonium sulfate, the real refractive indices of the mixtures are approximately the same as ammonium sulfate for all organic weight fractions. Various optical mixing rules for homogeneous and slightly heterogeneous systems fail to explain the experimental real refractive indices. It is likely that complex particle morphologies are responsible for the observed behavior of the mixed particles. Implications of our results for atmospheric modeling and aerosol structure are discussed.

## Introduction

The direct and indirect contributions of aerosols to radiative forcing remain the largest uncertainties in calculations of anthropogenic effects on climate.[1] The contribution of the aerosol direct effect to radiative forcing depends on the interaction of aerosols with radiation. Bulk refractive indices describe the amount of scattering and absorption of light by materials. When different compounds are combined to form internally mixed aerosols, the effective refractive indices are dependent on aerosol composition, shape, and structure. Obtaining these effective refractive indices will allow us to better characterize the aerosol direct effect.

Aerosols are composed of external and internal mixtures of multiple components including ammonium, nitrates, sulfates, and organics.[2] Observations of the ambient weight fraction of organic compounds range from 0.20 to 0.70.[2] The optical properties of aerosols have been explored to a limited extent in the literature in both laboratory[3−5] and field studies.[6,7] In laboratory studies of model anthropogenic aerosols, ammonium sulfate is often used as an inorganic salt due to its high propensity in tropospheric aerosols. Low molecular weight dicarboxylic acids are one of the most common organic components of tropospheric aerosols.[8] Primary sources for dicarboxylic acids include biomass burning and motor exhaust.[9,10] The oxidation of volatile and semivolatile organic compounds is also a source of dicarboxylic acids.[11]

Multiple optical mixing rules exist for determining the refractive indices of internally mixed systems. In the atmospheric literature, several different methods have been used. For homogeneous particles, volume-weighted refractive indices and weighting by the molar (or molal) refraction are considered.[4,12−14] The Maxwell−Garnett and the Bruggeman mixing rules deal with the refractive indices of heterogeneous particles.[15] In the Maxwell−Garnett mixing rule, particles are assumed to be composed of inclusions of one compound in a matrix of the other compound. The inclusions are assumed to be small, dilute, randomly distributed, and spherical. The Bruggeman approximation treats the inclusions and the matrix symmetrically so that the particles can be viewed as a completely random inhomogeneous medium where the individual components have similar properties to the inclusions in the Maxwell−Garnett mixing rule. One other optical mixing rule that can be considered is the dynamic effective medium approximation.[16,17] This optical mixing rule is the Bruggeman approximation with a higher-order term that accounts for the size distribution of the inclusions and the dependence of the optical properties on the size of the inclusions. Refractive indic results for nonabsorbing mixtures of glutaric acid and sodium chloride were compared to optical mixing rules in a study of Riziq et al.[4]

When an internal aerosol mixing state is incorporated into a global climate model, the most common way that aerosol optical properties are determined is by volume-weighting the refractive indices of aerosol constituents.[18,19] In one review of atmospheric models, dry aerosols composed of organic carbon are assumed to have real refractive indices of 1.53 and be weakly absorbing at 550 nm.[20] More complicated models such as the core−shell approximation and the dynamic effective medium approximation are sometimes used to treat internal mixtures of aerosols that contain black carbon.[17,19]

* To whom correspondence should be addressed. E-mail: tolbert@colorado.edu.
[†] CIRES.
[‡] Department of Atmospheric and Oceanic Sciences.
[§] Department of Chemistry and Biochemistry.
[#] Current address: Environmental Science and Engineering Program, California Institute of Technology, Pasadena, CA 91125.

10.1021/jp906240y CCC: $40.75 
Published on Web 10/30/2009

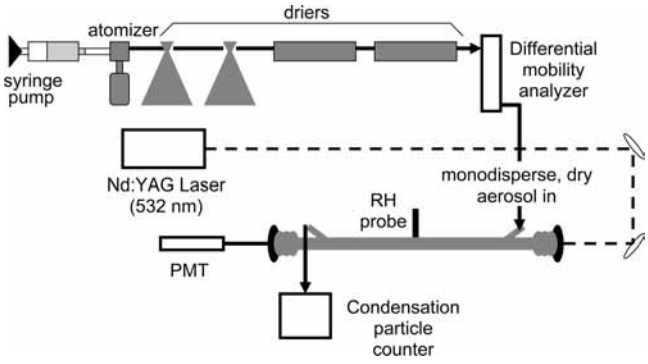


**Figure 1.** Schematic of the cavity ring-down aerosol extinction spectrometer.

**TABLE 1: Structure and Physical Properties of the Compounds Used in This Study**

| name | structure | density[a] (g/cm$^3$) | n[a] |
|---|---|---|---|
| oxalic acid | 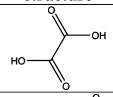 | 1.900 | --- |
| succinic acid | 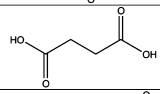 | 1.572 | 1.450 |
| adipic acid | 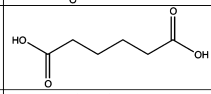 | 1.360 | --- |
| ammonium sulfate | $(NH_4)_2SO_4$ | 1.77 | 1.535[b] |
| sodium fluoride | NaF | 2.78 | 1.3252 |

[a] From ref 29 unless otherwise noted. Temperatures for the density measurements range from 17 to 25 °C. The real part of the refractive indices was measured at 589 nm. [b] From ref 28.

In this paper, we have explored the aerosol direct effect by investigating the optical properties of internal mixtures of dicarboxylic acids and ammonium sulfate. The less soluble dicarboxylic acids, oxalic, succinic, and adipic acids, were used. The optical properties of the aerosols were measured with cavity ring-down aerosol extinction spectroscopy (CRD-AES). We have found that small amounts of salt have a large effect on aerosol optical properties for these systems. Aerosol mass spectrometry (AMS) and Raman microscopy were used to determine aerosol composition, shape, and structure.

## Experimental Methods

Cavity ring-down aerosol extinction spectroscopy was used to measure particle extinction at 532 nm as a function of the organic weight fraction. Our system has been described in detail elsewhere,[21,22] so only a brief summary will be given here. A schematic of the instrument is shown in Figure 1.

A syringe pump and constant output atomizer (TSI 3076) were used to generate aerosols from aqueous solutions of the following compounds: oxalic acid (Sigma-Aldrich, 99+%, ACS reagent grade), succinic acid (Sigma-Aldrich, ≥99.0%, ACS reagent grade), adipic acid (Fluka, ≥99.5%), ammonium sulfate (Mallinckrodt Baker, ≥99.0%, ACS reagent grade), and sodium fluoride (Sigma-Aldrich, 99+%, ACS reagent grade). A list of the chemical structures and physical properties of the compounds is given in Table 1. Chemicals were used without further purification. Aqueous solutions that were approximately 0.05% by weight were made from one or more organic or inorganic components and HPLC-grade water (Honeywell, Fluka). Solutions were atomized using prepurified nitrogen at a flow rate of approximately 1.6 L/min.

Wet, polydisperse aerosols exiting the atomizer were dried using a series of four driers. The first two driers were 4 L Erlenmeyer flasks with activated alumina desiccant. The aerosol flow then proceeded through two diffusion driers (TSI 3062), containing molecular sieve and silica gel, respectively. A scanning mobility particle sizer (TSI 3080, 3081, 3022A) was used to characterize the aerosol distribution prior to the CRD-AES (not shown in Figure 1).

To measure aerosol optical properties, aerosols were size-selected using an electrostatic classifier (TSI 3080) and a differential mobility analyzer (DMA, TSI 3081) with a sheath flow of 5.0 L/min. Because we are size-selecting particles using a DMA, the diameters referred to throughout this paper are mobility diameters. The extinction of the monodisperse aerosol particles was measured at 532 nm using CRD-AES. A Nd:YAG laser is used to generate 532 nm light, which then enters a cavity that is approximately 85 cm long and is capped with highly reflective mirrors ($R > 99.998\%$). A photomultiplier tube is used to measure the decay of the intensity of the laser pulse with time. The characteristic ring-down time with no sample, $\tau_0$, is approximately 100 $\mu$s. When a sample is added, the ring-down time, $\tau$, decreases due to scattering and absorption of light by the sample material according to

$$I = I_0 \exp(-\alpha_{ext} h) \tag{1}$$

where $I$ is the intensity of light a distance $h$ away from an incident light with intensity $I_0$. The extinction $\alpha_{ext}$ has units of cm$^{-1}$. For the CRD-AES system, the difference in the ring-down times can be used to calculate the extinction, $\alpha_{ext}$ (cm$^{-1}$), which is given by

$$\alpha_{ext} = \frac{L_0}{L_S c}\left(\frac{1}{\tau} - \frac{1}{\tau_0}\right) \tag{2}$$

where $L_0$ is the length of the cavity, $L_S$ is the path length through the sample, and $c$ is the speed of light. The concentration of particles, $C$ (particles·cm$^{-3}$), is determined after the extinction measurement using a condensation particle counter (CPC, TSI 3022A). The extinction cross section, $\sigma_{ext}$, can then be calculated as

$$\sigma_{ext} = \frac{\alpha_{ext}}{C} \tag{3}$$

The refractive indices for a given mixture is found by comparing the experimentally obtained extinction to predictions from Mie scattering theory for each size of particle for which the extinction was measured. The Mie scattering regime is used because the wavelength of light (532 nm) is close to the size of the aerosol particles (250−550 nm). Because the DMA size-selects particles by their electrical mobility, most of the flow exiting the DMA is due to a monodisperse distribution of singly charged particles and a small population of a second monodisperse distribution of doubly charged particles with a larger diameter. The fraction of doubly charged particles is calculated and accounted for in the refractive indices retrieval.[23] Our flow conditions are chosen to minimize the number of doubly charged particles. Specifically, solution concentration and flow conditions were set in order to have a particle concentration of approximately $1 \times 10^3$ cm$^{-3}$ at a particle diameter of 100 nm and less than 5 cm$^{-3}$ at a diameter of 500 nm. In Figure 2, we have

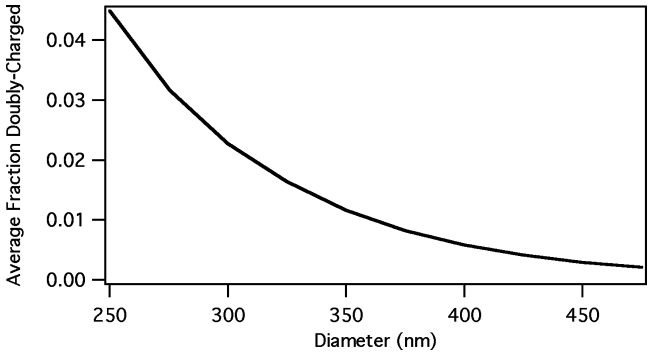


**Figure 2.** Average fraction of doubly charged particles as a function of the diameter of the corresponding singly charged particles for our experimental conditions. The average was taken over the data for the dicarboxylic acids, ammonium sulfate, and binary organic/inorganic mixtures.

plotted the mean number percentage of doubly charged particles averaged over all the dicarboxylic acid/ammonium sulfate refractive indices data in this paper. At the largest particle diameters, the mean number percentage of doubly charged particles becomes negligible.

The theoretical extinction efficiencies are determined for a range of real refractive indices and particle sizes using a spherical Mie code written for MATLAB that was adapted from Bohren and Huffman.[15,24] Because none of the compounds used absorb light at 532 nm, the imaginary refractive indices is fixed at zero. The calculated extinction efficiencies, $Q_{ext}$, are converted to extinction using the equation

$$\alpha_{ext} = Q_{ext}\pi r^2 C \tag{4}$$

where $r$ is the particle radius and $C$ is the concentration of particles in units of particles$\cdot$cm$^{-3}$ found from the CPC. The experimental and theoretical results are compared using a reduced cumulative fractional difference ($CFD_r$)

$$CFD_r = \frac{1}{N}\sum_{i=1}^{N}\frac{|\alpha_{ext(theory)} - \alpha_{ext(measured)}|}{\alpha_{ext(measured)}} \tag{5}$$

where $N$ is the number of sizes of particles used and the sum is taken over all sizes of particles for which the extinction is measured. The reduced $CFD_r$ is similar to $(\chi^2/N^2)^{1/2}$ (where $\chi^2$ has the usual definition) in that the minimum of both functions should occur at the same value of the domain. The theoretical refractive indices that gives the minimum $CFD_r$ is the refractive indices that best fits the data. We generally calculate $CFD_r$ values for $n = 1.2$ to $n = 1.8$ in increments of 0.001.

Complementary experiments were performed on the succinic acid/ammonium sulfate system to investigate the structure and composition of the aerosols using AMS and Raman microscopy. The AMS was used to determine the composition of aerosol particles that were generated, dried, and size-selected as for the cavity ring-down experiment. The AMS instrument has been described in detail in Allan et al., Jayne et al., and Jimenez et al.[25−27] Briefly, aerosol particles are focused through an aerodynamic lens while the airflow is pumped away to very high vacuum conditions. Particles are then vaporized when they hit a plate held at approximately 650 °C, and their components are ionized by electron impact ionization and analyzed with a quadrupole mass spectrometer. Higher weight percent solutions (1.0 wt %) were used in the AMS to obtain a sufficient number of particles.

For Raman microscopy, aerosols were imaged on quartz substrates. The substrates were treated with a commercial hydrophobic silanizing agent to produce a hydrophobic substrate and cleaned with methanol. Aerosol particles were generated and dried as in the cavity ring-down experiment. The dry aerosol flow was attached to a cascade impactor backed with an external pump to obtain supported particles for imaging.

The Raman microscope was used to determine aerosol shape and composition. An Olympus optical microscope with a 100× objective was used to detect the shape of the aerosol particles. An Almega Raman spectrometer was used to probe the chemical composition of individual aerosol particles. Incident light at 532 nm was used, and light that was scattered at 180° was detected. Higher weight percent solutions (1−15 wt %) were used to increase the number of particles with diameters larger than 1 $\mu$m.

## Results

The real refractive indices of internally mixed aerosols composed of dicarboxylic acids and ammonium sulfate were determined as a function of the organic weight fraction. We note, as in the Introduction, that refractive indices retrieved for aerosols may be better termed "effective refractive indices", as they depend on aerosol shape, composition, and structure. Three different dicarboxylic acids were used: oxalic, succinic, and adipic acid. Because the imaginary refractive indices of these compounds is zero at 532 nm, we will refer to refractive indices and the real part of the refractive indices interchangeably below. The chemical composition of the aerosol particles was determined from AMS and Raman microscopy. The aerosol shape and internal structure were investigated using optical and Raman microscopies.

To demonstrate the quality of the data obtained from the cavity ring-down technique, we show the experimental extinction cross sections for ammonium sulfate (Figure 3a) and succinic acid (Figure 3b) versus the theoretical extinction cross sections calculated using the bulk values for the refractive indices of these compounds. Theoretical cross sections are shown with and without the correction for the small percentage of doubly charged particles obtained during size selection by the DMA. The effect of this correction is most apparent for particles with smaller diameters due to the higher percentage of doubly charged particles. Even with the correction, a deviation between the data and the theory is observed for smaller diameters possibly due to higher-order, multiply charged particles. This result demonstrates excellent agreement with literature values for the pure compounds. The real refractive indices that we retrieve for ammonium sulfate is approximately 1.546, which is close to the bulk value of 1.535.[28] The experimentally obtained real refractive indices of pure succinic acid is 1.473, compared with the literature value for the bulk of 1.450.[29]

In Figure 4a, we show the real refractive indices for internal mixtures of oxalic acid and ammonium sulfate. The refractive indices are given by the minimum value of the $CFD_r$ as a function of refractive indices. A plot of $CFD_r$ values for representative oxalic acid and ammonium sulfate data is given in Figure 5. These curves show a single, well-defined minimum for each data set. For all of the refractive indices results, the data have been corrected to account for the distribution of doubly charged particles obtained during size-selection by the DMA.

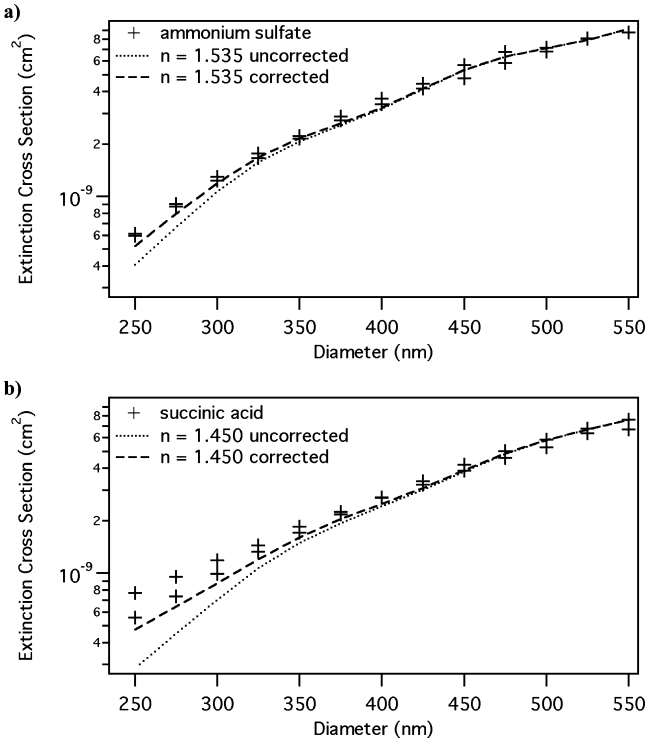


**Figure 3.** Experimental extinction cross sections for aerosol particles (+) compared to extinction cross sections calculated using literature values for the bulk materials (• • •) for (a) ammonium sulfate and (b) succinic acid. Theoretical extinction cross sections were also calculated accounting for the average experimentally determined contribution to the total concentration due to doubly charged particles (- - -).

The real refractive indices shown in Figures 4 and 6 were calculated using extinction data obtained for particles with diameters of 250−550 nm, measured in 25 nm diameter increments. Real refractive indices were also determined for data from diameters of 350−550 nm, again using 25 nm diameter increments. Two different ranges were used to examine the quality of our correction for doubly charged particles. The percent difference between the average refractive indices obtained with the two size ranges is less than 1.5% for all data presented in this paper. The experimentally derived real refractive indices of oxalic acid is 1.350. We were unable to find a literature value for pure oxalic acid. The refractive indices of aqueous oxalic acid were measured from 0.01 to 10 wt % by Myhre and Nielsen.[30] Using many different organic acids, including oxalic acid, they derive an empirical relation for the refractive indices at 633 nm of mixtures of one of more organic acids with water, which they state is valid for organic weight fractions of 0−0.6.[30] Extrapolating their results gives a refractive indices of 1.452 for pure organic acids, which agrees with our measurements for succinic and adipic acids, but is higher than either of our measurements for oxalic acid.

The data in Figure 4 are shown in comparison to the volume-weighted average refractive indices (solid line). This mixing rule is the simplest available to predict the refractive indices of mixtures of materials in which the components are evenly dispersed. This prediction is also commonly used in atmospheric models.[4,12−14] To calculate the volume-weighted average refractive indices, we use the equation

$$n_{vw} = \frac{V_{org}}{V_{tot}} n_{org} + \frac{V_{inorg}}{V_{tot}} n_{inorg} \quad (6)$$

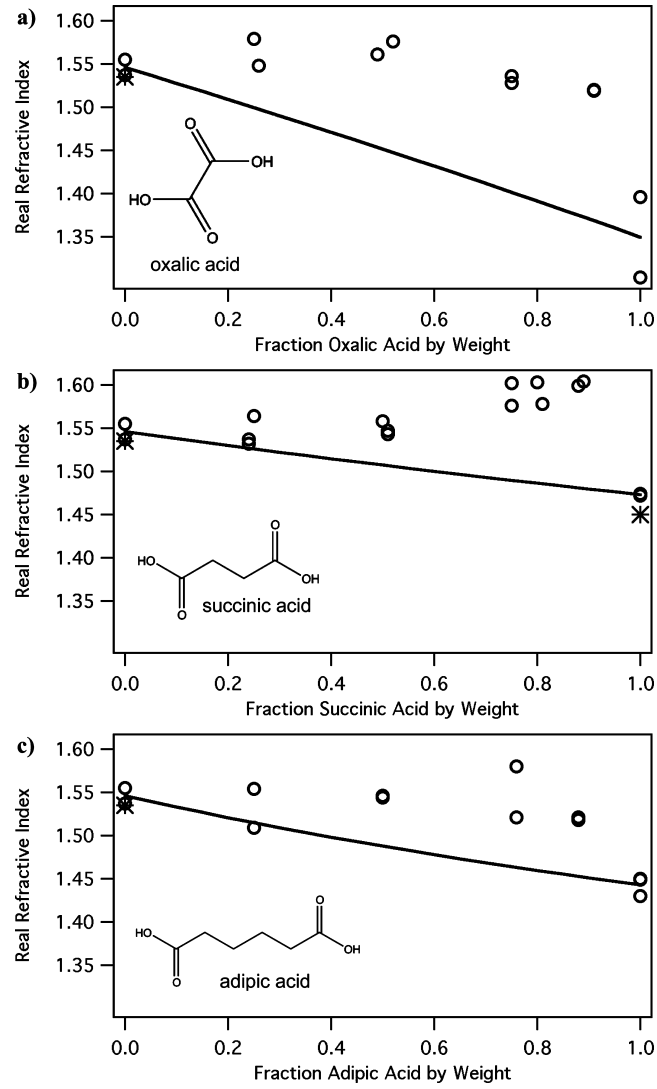


**Figure 4.** Real refractive indices of aerosol particles composed of ammonium sulfate and (a) oxalic acid, (b) succinic acid, and (c) adipic acid plotted as a function of the organic fraction by weight. The data (○) is compared to predicted refractive indices calculated by volume-weighting the experimentally determined refractive indices for the pure components (—). The literature real refractive indices for bulk ammonium sulfate and succinic acid are plotted for comparison (∗).

where $n_{vw}$, $n_{org}$, and $n_{inorg}$ are the real refractive indices for the volume-weighted average, the pure organic compound, and the pure inorganic compound; and $V_{org}$, $V_{inorg}$, and $V_{tot}$ are the volumes of the organic component, inorganic component, and total, respectively. We used the average experimental refractive indices for $n_{org}$ and $n_{inorg}$. The bulk densities of the two components were used to calculate the volume ratios for each weight fraction.

The experimentally derived refractive indices for the mixtures of oxalic acid and ammonium sulfate are similar to the values of pure ammonium sulfate for all mixtures. The volume-weighted refractive indices are much lower than the measured values. The data show that additions of small quantities of ammonium sulfate to the pure organic component can have a large effect on the refractive indices.

The real refractive indices derived for internal mixtures of succinic acid and ammonium sulfate are shown in Figure 4b in comparison to the prediction derived by volume-weighting the refractive indices. At an organic weight fraction of approximately 0.25, the real refractive indices is close to the

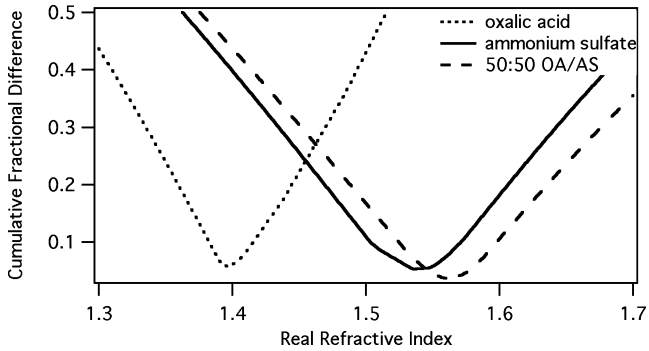


**Figure 5.** Sample refractive indices retrievals for three sets of extinction measurements. The reduced cumulative fractional difference ($CFD_r$) is plotted as a function of the refractive indices for oxalic acid (• • •), ammonium sulfate (—), and a mixture of oxalic acid and ammonium sulfate with an organic weight fraction of 0.5 (- - -). The minimum of each curve gives the retrieved refractive indices for that set of extinction measurements. In this case, the real refractive indices for oxalic acid, ammonium sulfate, and the mixture are 1.396, 1.537, and 1.561, respectively.

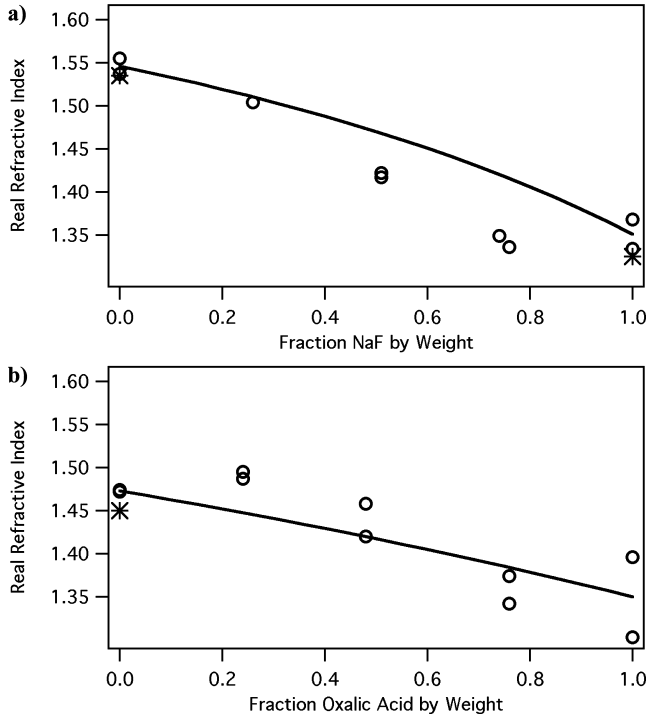


**Figure 6.** Same as Figure 4 for (a) sodium fluoride and ammonium sulfate mixtures and (b) oxalic acid and succinic acid mixtures. The literature values for the refractive indices of bulk ammonium sulfate, sodium fluoride, and succinic acid are plotted for comparison (∗).

volume-weighted prediction. At higher weight fractions, the refractive indices deviate from the prediction. When the organic weight fraction is 0.75−0.90, the real refractive indices of the mixtures are higher than either of the pure components.

The trends for the real refractive indices of internally mixed aerosols composed of adipic acid and ammonium sulfate are more similar to those for oxalic acid than succinic acid (Figure 4c). The real refractive indices of pure adipic acid was determined to be 1.443. The real refractive indices of each mixture are closer in value to the real refractive indices of ammonium sulfate than that of adipic acid.

In all cases, the data shown for mixtures of dicarboxylic acids and ammonium sulfate show positive deviations from the volume-weighted average refractive indices. Negative deviations have also been observed for other mixtures. Figure 6a shows refractive indices data that we obtained using CRD-AES for mixtures of the inorganic compound sodium fluoride with ammonium sulfate. Mixtures of sodium fluoride and ammonium sulfate have negative deviations from the volume-weighted refractive indices at high weight fractions of sodium fluoride. Note that we obtain a refractive indices of 1.351 for sodium fluoride, which is close to the literature value of 1.3252.[29] Figure 6b shows data for mixtures of two organic compounds, oxalic and succinic acids. In this case, the results are much closer to the volume-weighted prediction for all weight fractions.

There are several ways of estimating the error incurred in the extinction measurements and refractive indices retrieval. As stated above, the retrieved values for ammonium sulfate and succinic acid are approximately 0.02 higher than the literature values for the bulk materials. The error can also be estimated from the amount of scatter observed between data points at the same values of organic weight fraction. The average standard deviation in the real refractive indices for the data shown in Figure 4 is 0.015. This small standard deviation indicates that the observed positive deviations from the volume-weighted average refractive indices of the pure components are outside of experimental error.

To determine the cause of the unexpected refractive indices behavior observed, complementary experiments were performed on the succinic acid/ammonium sulfate system to address the assumptions inherent in our calculations of refractive indices. In particular, the chemical composition was determined through Raman microscopy and AMS. Optical and Raman microscopies were used to determine aerosol shape and structure.

AMS spectra of pure ammonium sulfate, pure succinic acid, and a mixture of succinic acid and ammonium sulfate at an organic weight fraction 0.50 are shown in Figure 7a. The mixture only has peaks originating from ammonium sulfate and succinic acid. In Figure 7b, the sum of the intensities of the most intense peaks due to succinic acid is shown versus the weight fraction of succinic acid for each mixture. A line is plotted showing the decrease in intensity that should occur between the pure succinic acid and each weight fraction. We show the results for 200 nm particles. The measured values show good agreement with the theoretical expectation for all diameters. The concentration of the atomized solution, therefore, is quite similar to the actual aerosol composition.

In Figure 8a, Raman scattering spectra are shown for pure ammonium sulfate, pure succinic acid, and a mixture of succinic acid and ammonium sulfate at an organic weight fraction of 0.25. Because of the small beam spot size of the instrument, we are able to acquire spectra of single aerosol particles on the quartz substrate, rather than spectra with contributions from multiple particles. The spectrum of the mixture is clearly a composite of the two components, demonstrating that the particles are internal mixtures of succinic acid and ammonium sulfate. Optical microscopy under a 100× objective shows that the particles are spherical (Figure 8b). Thus, the aerosol chemical composition and shape cannot explain the observed deviations from the volume-weighted average refractive indices prediction.

## Discussion

We obtain the literature values for the real refractive indices for the pure components within ±0.02. This result indicates the particles produced from the pure components are spherical, that the size selection of the electrostatic classifier is sufficiently monodisperse for the singly charged particles, and that we account for the small percentage of doubly charged particles

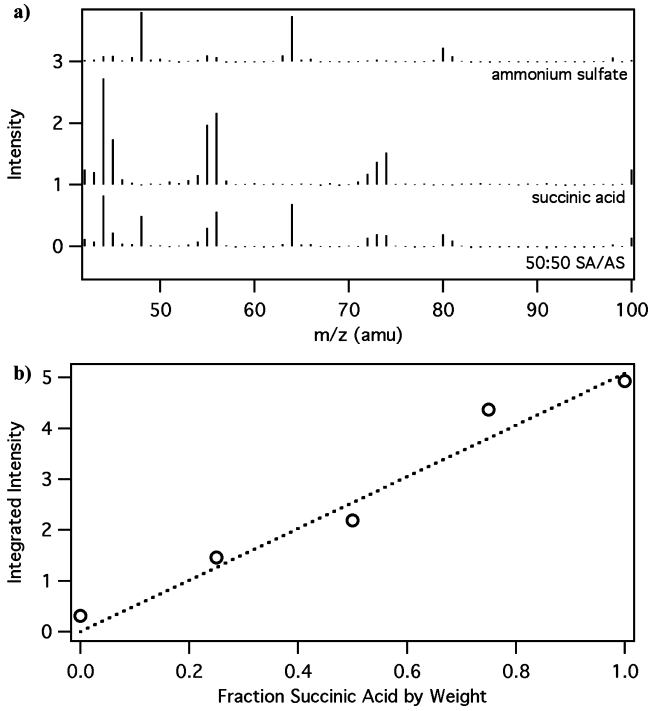


**Figure 7.** (a) AMS spectra of ammonium sulfate, succinic acid, and a mixture of succinic acid and ammonium sulfate at an organic weight fraction of 0.50. The spectra are offset for clarity. (b) The integrated intensity of the most intense peaks above 40 amu due to succinic acid (○) as a function of the fraction of succinic acid by weight. The theoretical decrease in intensity with decreases in weight fraction (- - -) is also shown. All AMS spectra in this figure are for particles of diameters of approximately 200 nm.

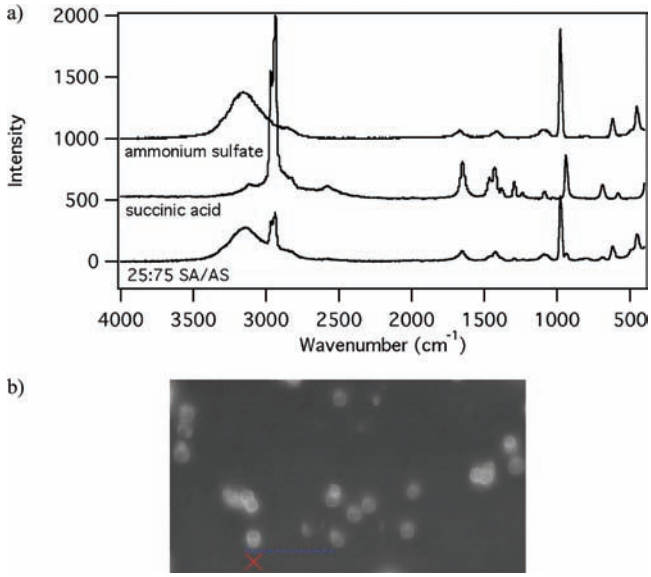


**Figure 8.** (a) Raman scattering spectra of ammonium sulfate, succinic acid, and a mixture of succinic acid and ammonium sulfate at an organic weight fraction of 0.25. The spectra are offset from one another for clarity. (b) An optical image of aerosol particles with an organic weight fraction of 0.25. The bottom spectrum in panel a is taken of the particle with the red x underneath it. The blue ruler indicates that the particle is approximately 2 $\mu$m in diameter.

sufficiently well. The Mie scattering calculations that are used to determine the refractive indices of the particles assume that the particles are spherical and monodisperse.

The refractive indices of the internal mixtures do not match the values obtained assuming that the refractive indices of the mixtures are volume-weighted averages of the pure components. Our results are similar to the raw data for glutaric acid and sodium chloride mixtures presented by Riziq et al.[4] If bulk densities are used in the calculation of the volume-weighted average refractive indices, their data also show positive deviations with respect to the theory. Deviations from the theory could be due to several experimental and theoretical reasons. For example, multiple optical mixing rules have been proposed.[4,15] Taking volume-weighted averages may not be the best optical mixing rule for these systems.

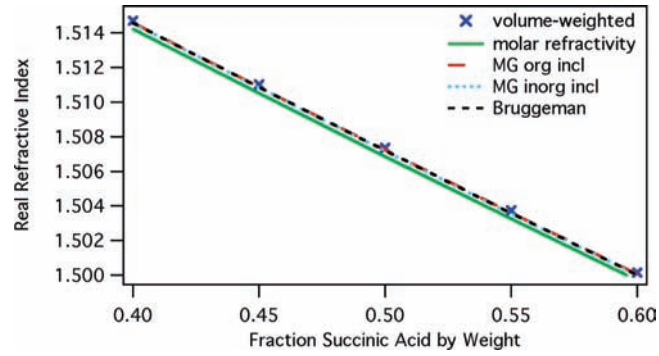


**Figure 9.** Comparison of the calculations performed using various optical mixing rules around an organic weight fraction of 0.5. The optical mixing rules include the volume-weighted average (×), weighting by the molar refractivity (—), Maxwell−Garnett with organic inclusions (— — —), Maxwell−Garnett with inorganic inclusions (• • •), and the Bruggeman approximation (- - -).

We have used a number of different optical mixing rules to compare our experimental results for the succinic acid and ammonium sulfate system to theoretical results for homogeneous particles and systems in which heterogeneities much smaller than Mie scatters are present. We have tried both volume-weighting the refractive indices and weighting by the molar refractivities of the pure components. The two models give slightly different values for the real refractive indices of the mixtures, but neither model fits the data. Assuming that the particles may have heterogeneities that are smaller than Mie scatters, we have applied the Maxwell−Garnett and Bruggeman mixing rules. For the Maxwell−Garnett approximation, we have assumed that the organic acid forms inclusions in a matrix of ammonium sulfate, which should be valid at low organic weight fractions. We also performed the calculation for ammonium sulfate inclusions in an organic acid matrix, which may hold for high organic weight fractions. For both regimes, deviations are seen from the volume-weighted average refractive indices, but these differences are not large enough to explain our results. The Bruggeman mixing rule is most appropriate for intermediate weight fractions. As for the Maxwell−Garnett approximation, the subtle deviations from the volume-weighted average refractive indices are not large enough to explain our results. The deviations are small for all weight fractions. In Figure 9, we show results for various optical mixing rules around an organic weight fraction of 0.5. Riziq et al. also applied the dynamic effective medium approximation to their system by using an average size for the inclusions, but the values obtained for nonabsorbing systems were similar to the other mixing rules.[4] Our results from these optical mixing rules suggest that the refractive indices we observed do not result from small heterogeneities in the particles. Simply adding a higher-order term to the Bruggeman approximation would not account for the significant difference observed between any of the optical mixing rules and the experimental data.

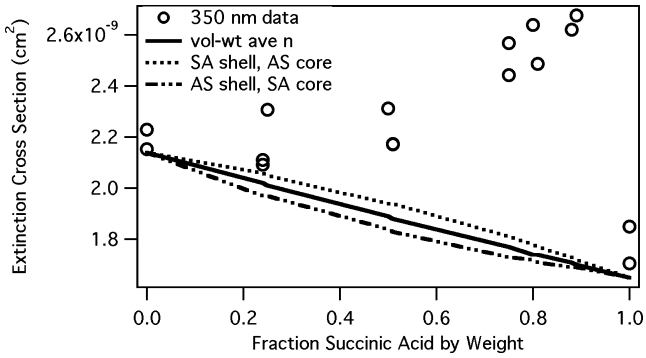


**Figure 10.** Extinction cross sections of succinic acid and ammonium sulfate mixtures (○) compared to theoretical extinction cross sections. Homogeneous particles with volume-weighted average refractive indices were used to determine extinction cross sections using a single-particle Mie scattering calculation (—). A core−shell Mie scattering calculation was used to determine extinction cross sections assuming a succinic acid shell and ammonium sulfate core (- - -) and an ammonium sulfate shell with a succinic acid core (— • • —). Extinction cross sections are shown for 350 nm particles.

The deviations from theory could be due to aerosol structure. If the particles were aspherical or fractal agglomerates, the refractive indices could change significantly. However, optical microscopy indicates the presence of spherical particles. Fractal agglomerates are not seen in the optical microscopy images. The particles, however, could potentially have heterogeneities that cannot be accounted for by the optical mixing rules discussed above due to core−shell or more complicated internal structures.

Using a version of the coated particle Mie code, bhcoat, adapted for MATLAB,[15,24] we have investigated whether the refractive indices obtained experimentally could result from core−shell structures rather than homogeneous structures or structures with small heterogeneities. Succinic acid has been shown to be surface active in a study of ternary mixtures of succinic acid with NaCl and $H_2O$.[31] This result suggests that the surface-active species, succinic acid, may partition to the aerosol−air interface forming a shell around the rest of the particle. In Figure 10, we show a comparison of experimental and theoretical extinction cross sections for the succinic acid/ammonium sulfate system. The experimental cross sections for 350 nm particles are shown. The cross sections are calculated directly from the data obtained for extinction and concentration. No correction has been performed to account for the small percentage of doubly charged particles. The theoretical cross sections are calculated using literature values for the refractive indices of succinic acid and ammonium sulfate. The literature densities of the bulk compounds are used to obtain the volume of succinic acid and ammonium sulfate at each organic weight fraction. From these volumes, the diameters of the core and the shell are calculated. The refractive indices and the diameters are the inputs to the core−shell Mie code. Three different theoretical cross sections are shown. The solid line shows the result when the calculation is performed assuming that the particles are homogeneous with refractive indices that result from volume-weighting the refractive indices of the pure components. The other refractive indices result from assuming that the particles have either an organic core with an inorganic coating or an inorganic core with an organic coating. We assume that if the core and the shell are not composed of pure components (for example, that the core is enhanced in the organic component, but also contains some inorganic material) the results for extinction should fall in between these two extremes. The results for the core−shell particles are close to that predicted for the homogeneous structures, however, and fail to explain the experimental results.

We have also considered other theoretical reasons that could explain our results. The refractive indices of a material has both real and imaginary components. In our analysis, we fixed the imaginary refractive indices to zero and determined the real refractive indices. The imaginary refractive indices accounts for the absorption of radiation by the particles. At an organic weight fraction of 0.75 for the succinic acid/ammonium sulfate system, the volume-weighted average refractive indices is 1.490, compared with the average experimental result of 1.589. For 350 nm particles, the same extinction efficiencies result for refractive indices of 1.589 + 0.00i and 1.490 + 0.59i. In other words, to explain the extinction by formation of an absorbing species would require an imaginary refractive indices of 0.59i, which for comparison, is significantly higher than has been found for the highly absorbing nigrosin dye (0.24i to 0.31i).[6,32] Ammonium sulfate and the dicarboxylic acids used in this study do not absorb at 532 nm, indicating that the imaginary refractive indices for the pure compounds is zero. The solutions we make are clear in color, and if we dry the aqueous mixtures in bulk, we obtain white crystals. We are therefore unlikely to be producing a solution that would be more strongly absorbing than nigrosin dye, which forms an opaque, black solution when dissolved at similar weight fractions. In the mass spectra of the particles and in Raman microscopy, there is no evidence for reactions between the compounds in the aerosol. An acid−base reaction between ammonium sulfate and succinic acid could, however, result in the formation of ammonium succinate. The refractive indices of ammonium succinate is unknown, but it is unlikely that this compound absorbs at 532 nm. If this compound forms in large quantities, we may be able to observe it in the Raman spectra. In the Raman spectrum of an internally mixed particle shown in Figure 8, we seem to observe peaks only due to succinic acid and ammonium sulfate. The spectrum of ammonium succinate, however, may be similar to the spectrum of succinic acid and ammonium sulfate mixtures. For example, the Raman spectra of ammonium sulfate and letovicite differ in peak intensities rather than peak positions.[33] As a result, it may be difficult to absolutely identify the mixture of compounds responsible for a spectrum. If a small quantity of material in the aerosol undergoes this reaction, the refractive indices may be slightly altered with no change in the Raman spectra. Our results may therefore in part be caused by the presence of ammonium succinate.

Our particles are produced from aqueous solution and then dried completely in a series of driers. The extinction of particles is measured at or below 10% RH. If the particles remain wet, then the composition of the particles will include organic, inorganic, and water components. If water is homogeneously distributed in the particle, then the refractive indices should be a volume-weighted average of the components. Since the refractive indices of water is 1.33, the addition of water would lower the refractive indices of the mixture if the components have higher refractive indices than water. If the particle forms a core−shell structure, calculations using ammonium sulfate and water show that the extinction efficiency decreases if water comprises the kernel or the shell of the particle. More complicated two component systems (for example, with a water−ammonium sulfate mixture as the core and a succinic acid shell) should produce similar results. Water contamination is therefore unlikely to cause our observed results. In addition,

no signal from water was observed in the Raman spectra of the pure or mixed compounds.

We have also considered the effect of organics on the phase behavior of ammonium sulfate to address the issue of the possible presence of water. Ammonium sulfate is known to deliquesce at 80% relative humidity (RH) and effloresce at 37% RH.[34] Pure succinic acid has an efflorescence relative humidity of 55−59% and a deliquescence relative humidity of above 94%.[35] The presence of organic acid, however, can alter the phase transitions of inorganic salts. For the ammonium sulfate/succinic acid system, a 1:1 mixture effloresces at 30−36% RH and deliquesces at 80% to >90% RH.[36] The deliquescence of the mixture is not uniform, with ammonium sulfate deliquescing at 80% RH and succinic acid remaining as solid inclusions in equilibrium with the aqueous component until 90% RH.[36] Our experimental procedure should therefore ensure that ammonium sulfate, succinic acid, and mixtures of varying weight percent are sufficiently dry.

The deviations in the refractive indices could result from a change in density in the mixed species. We have observed previously that the density of materials produced by the atomizer can be reduced compared to the bulk mixture, perhaps due to the inclusion of voids in the aerosol particle.[22,28] The reduction in density should, however, lower the refractive indices of the material. Density is also unlikely to be an issue because the deviations observed result in higher refractive indices than predicted regardless of whether the density of the dicarboxylic acid in question is higher or lower than that of ammonium sulfate. For example, oxalic acid has a higher density than ammonium sulfate, whereas succinic acid and adipic acid have lower densities than ammonium sulfate, but all the refractive indices results show positive deviations from the volume-weighted average.

The real refractive indices obtained may be caused by more complex structures than we have proposed above. Our calculation of extinction cross sections for particles with succinic acid shells and ammonium sulfate cores deviates from the extinction cross sections derived for homogeneous particles with volume-weighted refractive indices in the same direction as the experimental data. The magnitude of the deviations is not large enough to explain our experimental result. We have also shown from the optical mixing rules that small heterogeneities do not explain the experimental refractive indices. If larger heterogeneities were present and are large enough to be Mie scatterers in addition to the core−shell structure, we would expect to observe further deviations from the core−shell calculation. These more complex structures may explain our derived refractive indices.

Precedence for complex, phase-separated structures in particles exists in the literature of several fields. In the atmospheric literature, the formation of pores and phase separation occurring during particle drying has been discussed. For example, sodium chloride aerosols have been proposed to form solid particles with pockets of aqueous salt, maintaining a larger percentage of water than would be expected based on the relative humidity.[37] Numerous structures composed of polycrystalline domains with liquid cavities have been proposed for the $H_2SO_4/NH_3/H_2O$ system upon drying.[33] Because tropospheric aerosols take up and release water depending on the local relative humidity, these complex morphologies that form upon drying are likely to be atmospherically relevant. These complex structures that form upon solvent evaporation may be the cause of our refractive indices results. We plan to probe these systems directly using single-particle techniques such as atomic force and Raman microscopies to investigate whether complex internal structures are in fact present.

## Conclusions and Atmospheric Implications

We have measured the refractive indices of internally mixed aerosol particles composed of dicarboxylic acids with an even number of carbons and ammonium sulfate using CRD-AES. We obtain refractive indices for pure ammonium sulfate and pure dicarboxylic acids that are consistent with literature values, where they exist, to within experimental error. For mixtures, however, the experimental refractive indices do not match those of the volume-weighted average of the pure components. On the basis of comparisons of our results to multiple theories and data from complementary techniques, we conclude that the observed refractive indices may be due to complex particle internal structures.

Precedence exists in the literature for aerosol particles composed of internal mixtures of organic compounds and salts to have unexpected physical properties. For example, a small addition of salt to insoluble organics has been found to have a large impact on the ability of internally mixed particles to form cloud condensation nuclei.[38−41] The supersaturation required to activate the particles is higher than expected from traditional Köhler theory for 60 nm adipic acid particles containing up to 5 wt % NaCl and 80 nm succinic acid particles with up to 0.5 wt % NaCl.[38] The trend is more pronounced for smaller particles and less soluble species.[38]

Our results could have significant implications for atmospheric modeling. We have found, for internally mixed systems of ammonium sulfate and oxalic or adipic acid, that the refractive indices of the mixtures are close to the refractive indices of ammonium sulfate. Further investigation would have to be performed to determine if this effect can be generalized for other systems of nonabsorbing inorganic salts and organic acids. It would be interesting to determine whether generalizations could also be made for complex, more atmospherically relevant systems. Such generalizations, if they exist, may have the potential to greatly simplify atmospheric models. If a volume-weighted average is used, then the error between the calculation and the experimental refractive indices depends upon the refractive indices used for the organic component. In a review of aerosol modules for global circulation and transport models, the most common real refractive indices used for organic carbon is 1.53 at 550 nm.[20] Because ammonium sulfate also has a refractive indices of 1.53, the refractive indices calculated using these modules for internal mixtures of organic carbon and ammonium sulfate are consistent with our experimental results for oxalic and adipic acids. This coincidence results from the estimated real refractive indices of 1.53 chosen to describe organic compounds.

If species-specific refractive indices are used, rather than an average value for all organic carbon, then the deviation we observe from the volume-weighted average refractive indices could cause a significant difference in radiative forcing caused by dry particles. We can calculate for the succinic acid/ammonium sulfate data the difference in radiative forcing between the experimental refractive indices and the volume-weighted approximation using the approach given in Chylek and Wong.[42] We performed the calculation at an organic weight fraction of 0.75 with particles that are 350 nm in diameter and with particles having a Gaussian distribution peaking at a diameter of 60 nm with a standard deviation of 0.150. The experimental average real refractive indices of $n = 1.589$ at 532 nm gives a radiative forcing that is 1.4 times larger than

the volume-weighted average refractive indices of $n = 1.490$. This result indicates that there is significantly more light scattering predicted from our experimental result than from the volume-weighted approximation, which would cause greater atmospheric cooling. We note that when water is added as an aerosol component, possible differences in dry aerosol refractive indices are greatly reduced due to the volume of water in the particles. When aerosol particles encounter areas of low relative humidity, however, they may form complex microstructures upon drying resulting in refractive indices that deviate from traditional optical mixing rules. The expected radiative forcing based on the volume-weighted average refractive indices therefore may be different than the actual forcing calculated from experimentally derived refractive indices. Accounting for these differences in particle morphology and refractive indices would help to reduce the uncertainty in the aerosol direct effect.

**Acknowledgment.** The authors are grateful to K. J. Baustian for the Raman spectrum and D. O. De Haan, H. L. DeWitt, and M. G. Trainer for help and training on the AMS. This work was supported primary through NASA Grant Nos. NNG06GE79G and NNX09AE12G. Partial support was also received from NSF-ATM-0650023. M.A.F. acknowledges support from the NOAA Climate and Global Change Postdoctoral Fellowship Program administered by the University Corporation for Atmospheric Research. C.A.H. is supported through the NSF Graduate Research Fellowship Program. M.R.B. was supported by an EPA STAR graduate research fellowship (FP-91654601). The research described in this paper has been funded in part by the United States Environmental Protection Agency (EPA) under the Science to Achieve Results (STAR) Graduate Fellowship Program. EPA has not officially endorsed this publication, and the views expressed herein may not reflect the views of the EPA.

## References and Notes

(1) Solomon, S., Qin, D., Manning, M., Chen, Z., Marquis, M., Averyt, K. B., Tignor, M., Miller, H. L., Eds.; *Intergovernmental Panel on Climate Change, Climate Change 2007: The Physical Science Basis*; Cambridge University Press: New York, 2007.

(2) Zhang, Q.; et al, *Geophys. Res. Lett.* **2007**, *34*, L13801. DOI: 10.1029/2007GL029979.

(3) Pettersson, A.; Lovejoy, E. R.; Brock, C. A.; Brown, S. S.; Ravishankara, A. R. *J. Aerosol Sci.* **2004**, *35*, 995–1011.

(4) Riziq, A. A.; Erlick, C.; Dinar, E.; Rudich, Y. *Atmos. Chem. Phys.* **2007**, *7*, 1523–1536.

(5) Riziq, A. A.; Trainic, M.; Erlick, C.; Segre, E.; Rudich, Y. *Atmos. Chem. Phys.* **2008**, *8*, 1823–1833.

(6) Dinar, E.; Riziq, A. A.; Spindler, C.; Erlick, C.; Kiss, G.; Rudich, Y. *Faraday Discuss.* **2008**, *137*, 279–295.

(7) Massoli, P.; Bates, T. S.; Quinn, P. K.; Lack, D. A.; Baynard, T.; Lerner, B. M.; Tucker, S. C.; Brioude, J.; Stohl, A.; Williams, E. J. *J. Geophys. Res.* **2009**, *114*, D00F07. DOI: 10.1029/2008JD011604.

(8) Kawamura, K.; Umemoto, N.; Mochida, M.; Bertram, T.; Howell, S.; Huebert, B. J. *J. Geophys. Res.* **2003**, *108* (D23), 8639. DOI: 10.1029/2002jd003256.

(9) Narukawa, M.; Kawamura, K.; Takeuchi, N.; Nakajima, T. *Geophys. Res. Lett.* **1999**, *26* (20), 3101–3104.

(10) Kawamura, K.; Kaplan, I. R. *Environ. Sci. Technol.* **1987**, *21*, 105–110.

(11) Kawamura, K.; Kasukabe, H.; Barrie, L. A. *Atmos. Environ.* **1996**, *30* (10−11), 1709–1722.

(12) Jacobson, M. Z. *J. Geophys. Res.* **2002**, *107* (D19), 4366. DOI: 10.1029/2001jd002044.

(13) Stelson, A. W. *Environ. Sci. Technol.* **1990**, *24* (11), 1676–1679.

(14) Tang, I. N. *J. Geophys. Res.* **1997**, *102* (D2), 1883–1893.

(15) Bohren, C. F.; Huffman, D. R. *Absorption and Scattering of Light by Small Particles*; Wiley-VCH: Weinheim, Germany, 2004.

(16) Chylek, P.; Ramaswamy, V.; Cheng, R. J. *J. Atmos. Sci.* **1984**, *41* (21), 3076–3084.

(17) Jacobson, M. Z. *J. Phys. Chem. A* **2006**, *110*, 6860–6873.

(18) Stier, P.; Seinfeld, J. H.; Kinne, S.; Boucher, O. *Atmos. Chem. Phys.* **2007**, *7*, 5237–5261.

(19) Zhang, Y. *Atmos. Chem. Phys.* **2008**, *8*, 2895–2932.

(20) Kinne, S.; et al, *J. Geophys. Res.* **2003**, *108* (D20), 4634. DOI: 10.1029/2001jd001253.

(21) Baynard, T.; Lovejoy, E. R.; Pettersson, A.; Brown, S. S.; Lack, D.; Osthoff, H.; Massoli, P.; Ciciora, S.; Dube, W. P.; Ravishankara, A. R. *Aerosol Sci. Technol.* **2007**, *41*, 447–462.

(22) Beaver, M. R.; Garland, R. M.; Hasenkopf, C. A.; Baynard, T.; Ravishankara, A. R.; Tolbert, M. A. *Environ. Res. Lett.* **2008**, *3*, 045003.

(23) Weidensohler, A. *J. Aerosol Sci.* **1988**, *19* (3), 387–389.

(24) Mätzler, C. IAP Research Report, No. 2002-08 [Online]; Universität Bern: Bern, Switzerland, 2002. http://diogenes.iwt.unibremen.de/vt/laser/wriedt/Mie_Type_Codes/body_mie_type_codes.html (accessed May 2008).

(25) Allan, J. D.; Jimenez, J. L.; Williams, P. I.; Alfarra, M. R.; Bower, K. N.; Jayne, J. T.; Coe, H.; Worsnop, D. R. *J. Geophys. Res.* **2003**, *108* (D3), 4090. DOI: 10.1029/2002JD002358.

(26) Jayne, J. T.; Leard, D. C.; Zhang, X.; Davidovits, P.; Smith, K. A.; Kolb, C. E.; Worsnop, D. R. *Aerosol Sci. Technol.* **2000**, *33* (1−2), 49–70.

(27) Jimenez, J. L.; et al, *J. Geophys. Res.* **2003**, *108* (D7), 8425. DOI: 10.1029/2001JD001213.

(28) Garland, R. M.; Ravishankara, A. R.; Lovejoy, E. R.; Tolbert, M. A.; Baynard, T. *J. Geophys. Res.* **2007**, *112*, D19303. DOI: 10.1029/2006JD008179.

(29) Lide, D. R., Ed. *CRC Handbook of Chemistry and Physics*, 89th ed. [Online]; CRC Press/Taylor and Francis: Boca Raton, FL, 2009.

(30) Myhre, C. E. L.; Nielsen, C. J. *Atmos. Chem. Phys.* **2004**, *4*, 1759–1769.

(31) Vanhanen, J.; Hyvärinen, A.-P.; Anttila, T.; Raatikainen, T.; Viisanen, Y.; Lihavainen, H. *Atmos. Chem. Phys.* **2008**, *8*, 4595–4604.

(32) Lack, D. A.; Lovejoy, E. R.; Baynard, T.; Pettersson, A.; Ravishankara, A. R. *Aerosol Sci. Technol.* **2006**, *40*, 697–708.

(33) Colberg, C. A.; Krieger, U. K.; Peter, T. *J. Phys. Chem. A* **2004**, *108*, 2700–2709.

(34) Tang, I. N.; Fung, K. H.; Imre, D. G.; Munkelwitz, H. R. *Aerosol Sci. Technol.* **1995**, *23*, 443–453.

(35) Peng, C.; Chan, M. N.; Chan, C. K. *Environ. Sci. Technol.* **2001**, *35*, 4495–4501.

(36) Ling, T. Y.; Chan, C. K. *J. Geophys. Res.* **2008**, *113*, D14205. DOI: 10.1029/2008JD009779.

(37) Weis, D. D.; Ewing, G. E. *J. Geophys. Res.* **1999**, *104* (D17), 21275–21285.

(38) Bilde, M.; Svenningsson, B. *Tellus* **2004**, *56B*, 128–134.

(39) Broekhuizen, K.; Kumar, P. P.; Abbatt, J. P. D. *Geophys. Res. Lett.* **2004**, *31*, L01107. DOI: 10.1029/2003gl018203.

(40) Raymond, T. M.; Pandis, S. N. *J. Geophys. Res.* **2003**, *108* (D15), 4469. DOI: 10.1029/2003jd003503.

(41) Shantz, N. C.; Leaitch, W. R.; Caffrey, P. F. *J. Geophys. Res.* **2003**, *108* (D5), 4168. DOI: 10.1029/2002jd002540.

(42) Chylek, P.; Wong, J. *Geophys. Res. Lett.* **1995**, *22* (8), 929–931.

JP906240Y